Verified Calculation of Multiscale Combustion in Gaseous Mixtures

Joseph M. Powers

Department of Aerospace & Mechanical Engineering

Department of Applied & Computational Mathematics & Statistics

University of Notre Dame

Notre Dame, Indiana, USA

delivered to

Stanford University

1 August 2011

Acknowledgments

- Samuel Paolucci, U. Notre Dame
- Ashraf al-Khateeb, Khalifa U.
- Zach Zikoski, Ph.D. student, U. Notre Dame
- Christopher Romick, Ph.D. student, U. Notre Dame
- Stephen Voelkel, NSF-REU undergraduate student, U. Notre Dame
- Karel Matouš, U. Notre Dame
- National Science Foundation
- NASA

Outline

- Part I: Preliminaries
- Part II: Fundamental linear analysis of length scales of reacting flows with detailed chemistry and multicomponent transport.
- Part III: Direct Numerical Simulation (DNS) of complex inert and reactive flows with a wavelet-based adaptive algorithm implemented in a massively parallel computing architecture.

Part I: Preliminaries

Some Semantics

- *Verification*: Solving the equations right—a math exercise.
- *Validation*: Solving the right equations—a physics exercise.
- *DNS*: a verified and validated computation that resolves *all* ranges of relevant continuum physical scales present.

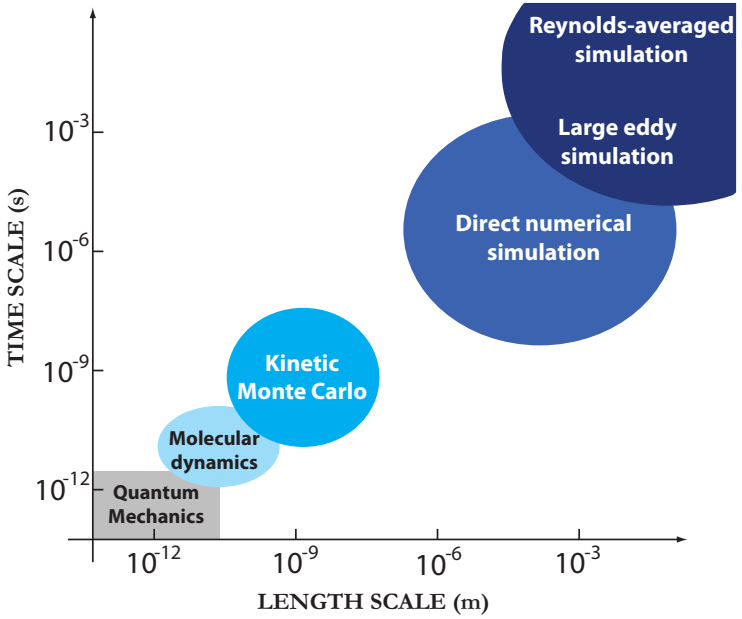

"Research needs for future internal combustion engines," *Phys. Today, 2008.*

Hypothesis

DNS of fundamental compressible reactive flow fields (thus, detailed kinetics, viscous shocks, multi-component diffusion, etc. are represented, verified, and validated) is on a trajectory toward realization via advances in

- adaptive refinement algorithms, and
- massively parallel architectures.

Corollary I

A variety of modeling compromises, e.g.

- shock-capturing (FCT, PPM, ENO, WENO, etc.),
- implicit chemistry with operator splitting,
- low Mach number approximations,
- turbulence modeling (RANS, $k - \epsilon$, LES, etc.), or
- reduced/simplified kinetics, flamelet models,

need not be invoked *when and if* this difficult goal of DNS is realized; **simple low order explicit discretizations suffice if spatio-temporal grid resolution is achieved.**

Corollary II

Micro-device level DNS is feasible today; macro-device level DNS remains in the distant future.

Corollary III

A variety of challenging fundamental unsteady multi-dimensional compressible reacting flows are now becoming amenable to DNS, especially in the weakly unstable regime; **we would do well as a community to direct more of our efforts towards *unfiltered* simulations so as to more starkly expose the richness of unadulterated continuum scale physics.**

[Example (only briefly shown today): ordinary WENO shock-capturing applied to unstable detonations can dramatically corrupt the long time limit cycle behavior; retention of physical viscosity allows relaxation to a unique dissipative structure in the unstable regime.]

Part II: Fundamental Linear Analysis of Length Scales

Motivation

- To achieve DNS, the interplay between chemistry and transport needs to be captured.
- The interplay between reaction and diffusion length and time scales is well summarized by the classical formula

$$\ell \sim \sqrt{D\,\tau}.$$

- Segregation of chemical dynamics from transport dynamics is a prevalent notion in reduced kinetics combustion modeling.
- But, can one rigorously mathematically verify an NS model without resolving the small length scale induced by fast reaction? *Answer: no.*
- Do micro-scales play a role in macro-scale non-linear dynamics? *Answer: in some cases, yes*, see Romick, Aslam, & Powers, 2011.

Illustrative Linear Model Problem

A linear one-species, one-dimensional unsteady model for reaction, advection, and diffusion:

$$\frac{\partial \psi}{\partial t} + u\frac{\partial \psi}{\partial x} = D\frac{\partial^2 \psi}{\partial x^2} - a\psi,$$

$$\psi(0,t) = \psi_u, \quad \left.\frac{\partial \psi}{\partial x}\right|_{x=\mathtt{L}} = 0, \qquad \psi(x,0) = \psi_u.$$

Time scale spectrum

For the spatially homogenous version: $\psi_h(t) = \psi_u \exp(-at)$,

reaction time constant: $\tau = \dfrac{1}{a} \implies \Delta t \ll \tau.$

Length Scale Spectrum

- The steady structure:

$$\psi_s(x) = \psi_u \left(\frac{\exp(\mu_1 x) - \exp(\mu_2 x)}{1 - \frac{\mu_1}{\mu_2} \exp(\mathrm{L}(\mu_1 - \mu_2))} + \exp(\mu_2 x) \right),$$

$$\mu_1 = \frac{u}{2D} \left(1 + \sqrt{1 + \frac{4aD}{u^2}} \right), \qquad \mu_2 = \frac{u}{2D} \left(1 - \sqrt{1 + \frac{4aD}{u^2}} \right),$$

$$\ell_i = \left| \frac{1}{\mu_i} \right|.$$

- For fast reaction ($a \gg u^2/D$):

$$\ell_1 = \ell_2 = \sqrt{\frac{D}{a}} = \sqrt{D\tau} \implies \Delta x \ll \sqrt{D\tau}.$$

Spatio-Temporal Spectrum

$$\psi(x,t) = \Psi(t)e^{\mathbf{i}kx} \quad \Rightarrow \quad \Psi(t) = C\exp\left(-a\left(1+\frac{\mathbf{i}ku}{a}+\frac{Dk^2}{a}\right)t\right).$$

- For long length scales: $\lim_{k\to 0}\tau = \lim_{\lambda\to\infty}\tau = \frac{1}{a},$
- For fine length scales: $\lim_{k\to\infty}\tau = \lim_{\lambda\to 0}\tau = \frac{\lambda^2}{4\pi^2}\frac{1}{D},$

$$\Bigg\} \quad \mathcal{S}_t = \left(\frac{2\pi}{\lambda}\sqrt{\frac{D}{a}}\right)^2.$$

- Balance between reaction and diffusion at $k \equiv \frac{2\pi}{\lambda} = \sqrt{\frac{a}{D}} = 1/\ell,$

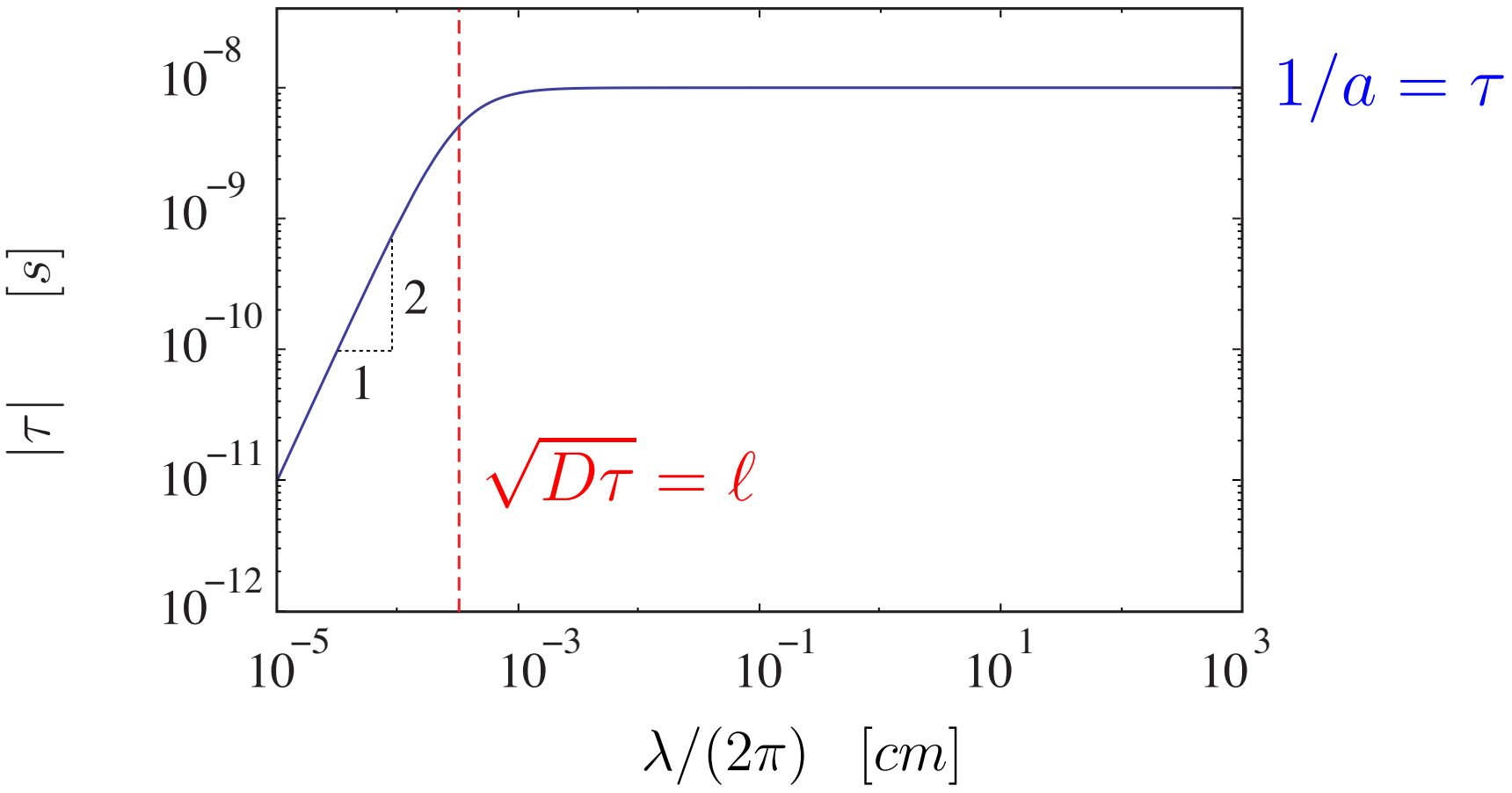

- Similar to $H_2 - air$: $\tau = 1/a = 10^{-8}\ s, D = 10\ cm^2/s,$
- $\ell = \sqrt{\frac{D}{a}} = \sqrt{D\tau} = 3.2 \times 10^{-4}\ cm.$

Laminar Premixed Flames

Adopted Assumptions:

- One-dimensional,
- Low Mach number,
- Neglect thermal diffusion effects and body forces.

Governing Equations:

$$\frac{\partial \rho}{\partial t} + \frac{\partial}{\partial x}(\rho u) = 0,$$

$$\rho \frac{\partial h}{\partial t} + \rho u \frac{\partial h}{\partial x} + \frac{\partial j^q}{\partial x} = 0,$$

$$\rho \frac{\partial y_l}{\partial t} + \rho u \frac{\partial y_l}{\partial x} + \frac{\partial j_l^m}{\partial x} = 0, \quad l = 1, \ldots, L-1,$$

$$\rho \frac{\partial Y_i}{\partial t} + \rho u \frac{\partial Y_i}{\partial x} + \frac{\partial j_i^m}{\partial x} = \dot{\omega}_i \bar{m}_i, \quad i = 1, \ldots, N-L.$$

- Unsteady spatially homogeneous reactive system:

$$\frac{d\mathbf{z}(t)}{dt} = \mathbf{f}\left(\mathbf{z}(t)\right), \qquad \mathbf{z}(t) \in \mathbb{R}^N, \quad \mathbf{f} : \mathbb{R}^N \rightarrow \mathbb{R}^N.$$

$$\mathbf{0} = (\mathbf{J} - \lambda \mathbf{I}) \cdot \boldsymbol{v}.$$

$$\mathcal{S}_t = \frac{\tau_{slowest}}{\tau_{fastest}}, \quad \tau_i = \frac{1}{|Re(\lambda_i)|}, \qquad i = 1, \ldots, R \leq N - L.$$

- Steady spatially inhomogeneous reactive system:

$$\tilde{\mathbf{B}}\left(\tilde{\mathbf{z}}(x)\right) \cdot \frac{d\tilde{\mathbf{z}}(x)}{dx} = \tilde{\mathbf{f}}\left(\tilde{\mathbf{z}}(x)\right), \qquad \tilde{\mathbf{z}}(x) \in \mathbb{R}^{2N+2}, \quad \tilde{\mathbf{f}} : \mathbb{R}^{2N+2} \rightarrow \mathbb{R}^{2N+2}.$$

$$\tilde{\lambda}\tilde{\mathbf{B}} \cdot \tilde{\boldsymbol{v}} = \tilde{\mathbf{J}} \cdot \tilde{\boldsymbol{v}}.$$

$$\mathcal{S}_x = \frac{\ell_{coarsest}}{\ell_{finest}}, \quad \ell_i = \frac{1}{|Re(\tilde{\lambda}_i)|}, \qquad i = 1, \ldots, 2N - L.$$

Laminar Premixed Hydrogen–Air Flame

- Standard detailed mechanism[a]; $N = 9$ species, $L = 3$ atomic elements, and $J = 19$ reversible reactions,
- stoichiometric hydrogen-air: $2H_2 + (O_2 + 3.76N_2)$,
- adiabatic and isobaric: $T_u = 800\ K,\ p = 1\ atm$,
- calorically imperfect ideal gases mixture,
- neglect Soret effect, Dufour effect, and body forces,
- CHEMKIN and IMSL are employed.

---

[a] J. A. Miller, R. E. Mitchell, M. D. Smooke, and R. J. Kee, *Proc. Combust. Ins.* **19**, p. 181, 1982.

- Unsteady spatially homogeneous reactive system:

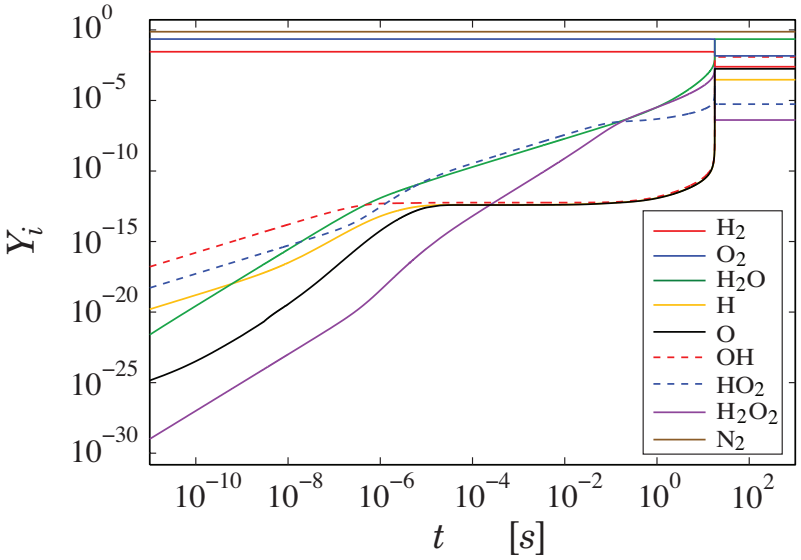

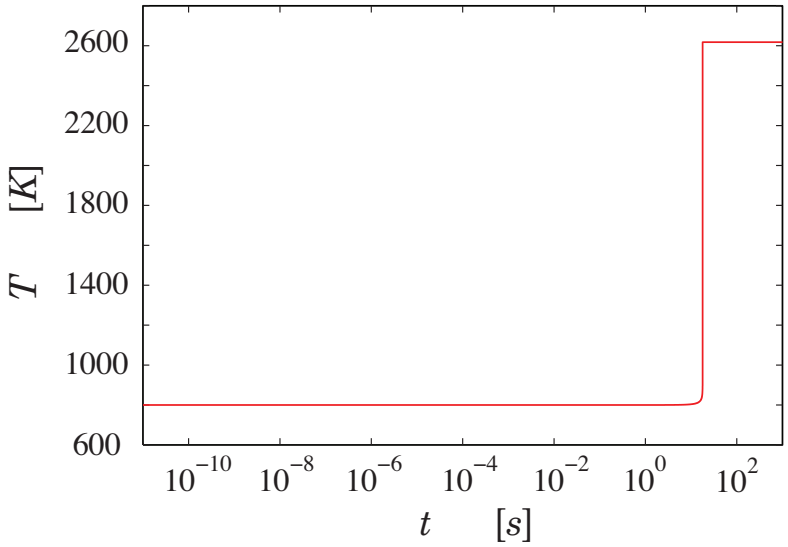

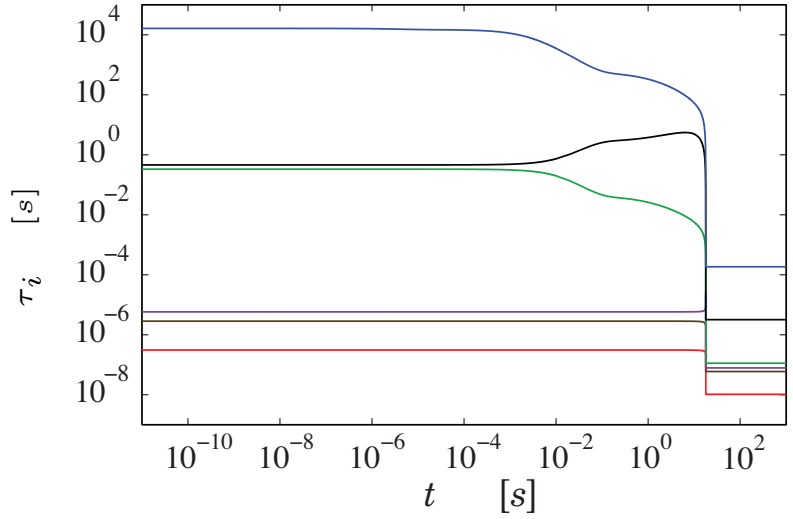

$\tau_{slowest} = 1.8\times10^{-2}\ s$

$\tau_{fastest} = 1.0\times10^{-8}\ s$

$\mathcal{S}_t \sim \mathcal{O}\left(10^4\right).$

- Steady spatially inhomogeneous reactive system:[a]

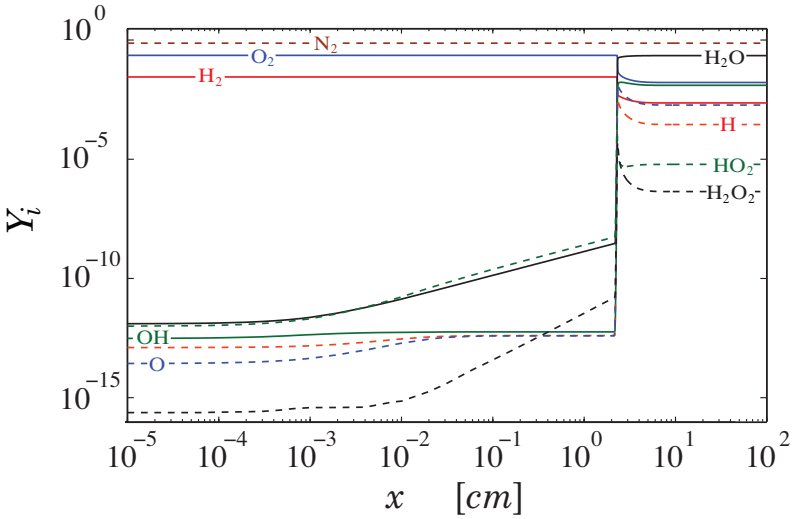

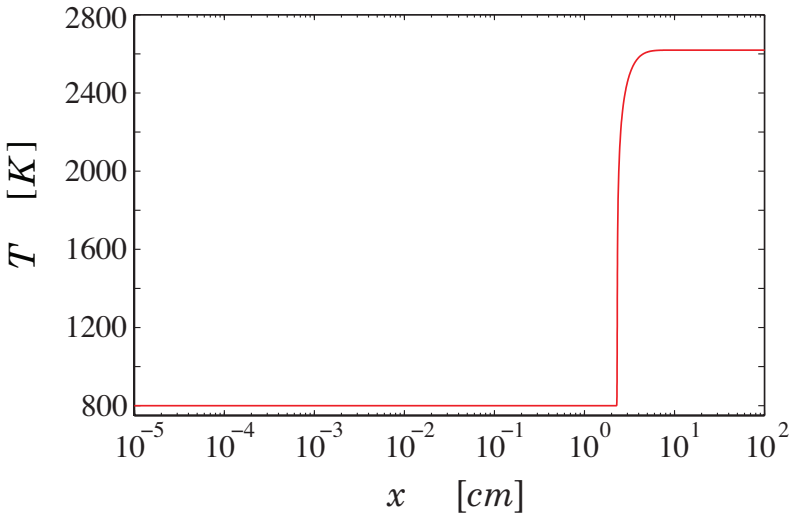

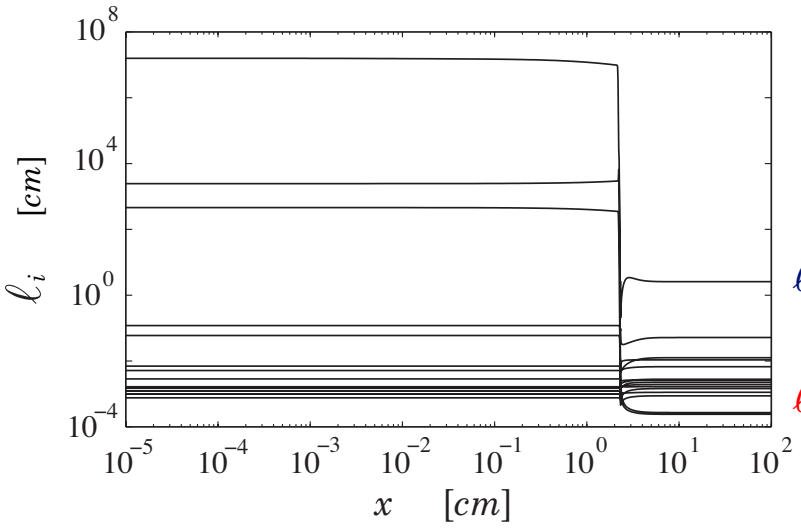

$\ell_{coarsest} = 2.6\times10^{0}\ cm$

$\ell_{finest} = 2.4\times10^{-4}\ cm$

$\mathcal{S}_x \sim \mathcal{O}\left(10^4\right).$

[a] A. N. Al-Khateeb, J. M. Powers, and S. Paolucci, *Comm. Comp. Phys.* 8(2): 304, 2010.

Spatio-Temporal Spectrum

- PDEs $\longrightarrow$ $2N+2$ PDAEs,

$$\mathbf{A}(\mathbf{z}) \cdot \frac{\partial \mathbf{z}}{\partial t} + \mathbf{B}(\mathbf{z}) \cdot \frac{\partial \mathbf{z}}{\partial x} = \mathbf{f}(\mathbf{z}).$$

- Spatially homogeneous system at chemical equilibrium subjected to a spatially inhomogeneous perturbation, $\mathbf{z}' = \mathbf{z} - \mathbf{z}^e$,

$$\mathbf{A}^e \cdot \frac{\partial \mathbf{z}'}{\partial t} + \mathbf{B}^e \cdot \frac{\partial \mathbf{z}'}{\partial x} = \mathbf{J}^e \cdot \mathbf{z}'.$$

- Spatially discretized spectrum,

$$\boldsymbol{\mathcal{A}}^e \cdot \frac{d\boldsymbol{\mathcal{Z}}}{dt} = (\boldsymbol{\mathcal{J}}^e - \boldsymbol{\mathcal{B}}^e) \cdot \boldsymbol{\mathcal{Z}}, \qquad \boldsymbol{\mathcal{Z}} \in \mathbb{R}^{2\mathcal{N}(N+1)}.$$

- The time scales of the generalized eigenvalue problem,

$$\tau_i = \frac{1}{|Re\,(\lambda_i)|}, \quad i = 1, \ldots, (\mathcal{N}-1)(N-1).$$

- $D_{mix} = \frac{1}{N^2} \sum_{i=1}^{N} \sum_{j=1}^{N} \mathfrak{D}_{ij}$,
- $\ell_1 = \sqrt{D_{mix} \tau_s} = 1.1 \times 10^{-1}\ cm$,
- $\ell_2 = \sqrt{D_{mix} \tau_f} = 8.0 \times 10^{-4}\ cm \approx \ell_{finest} = 2.4 \times 10^{-4}\ cm$.

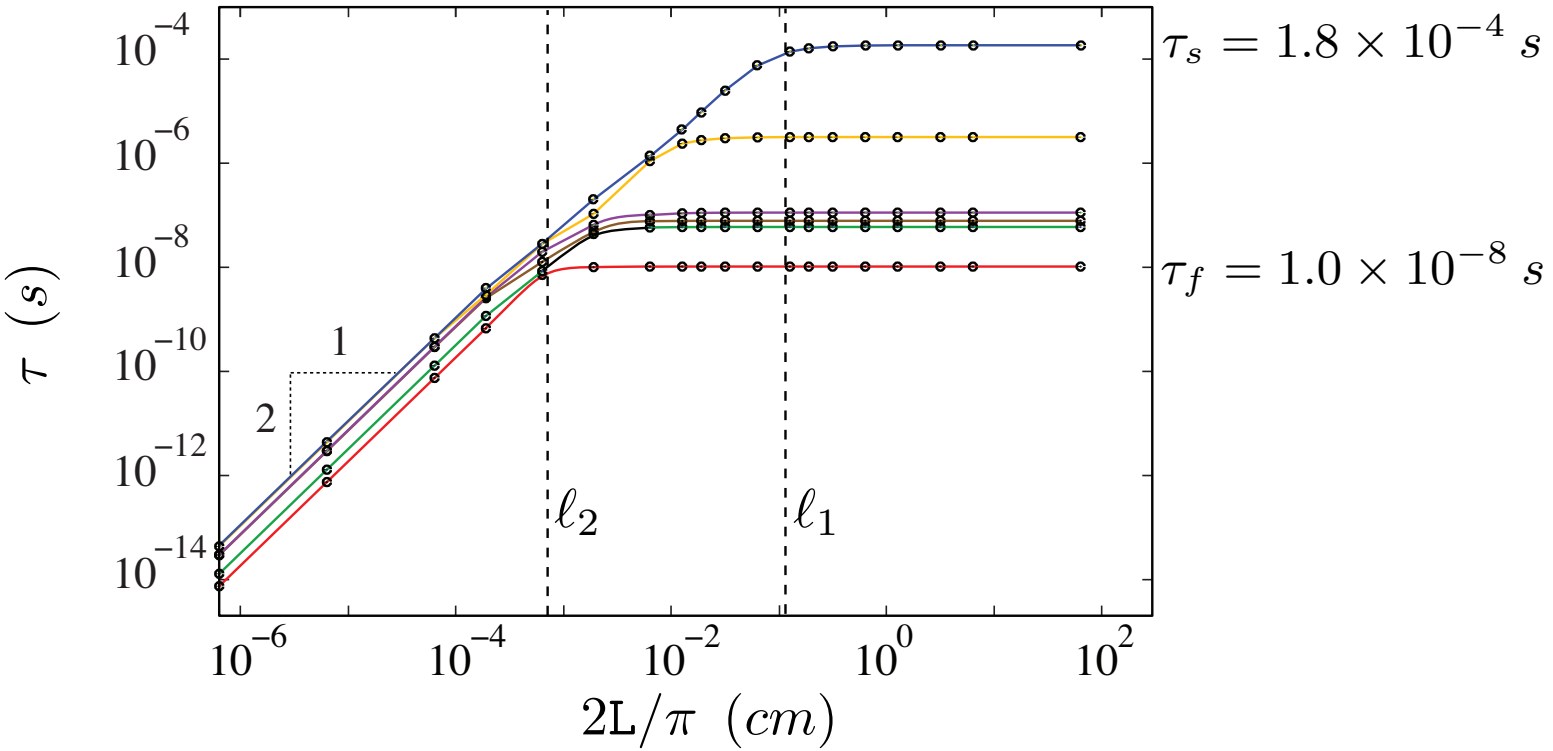

Conclusions: Part I

- Time and length scales are coupled.
- Coarse wavelength modes have time scales dominated by reaction.
- Short wavelength modes have time scales dominated by diffusion.
- Fourier modal analysis reveals a cutoff length scale for which time scales are dictated by a balance between transport and chemistry.
- Fine scales, temporal and spatial, are essential to resolve reacting systems; the finest length scale is related to the finest time scale by $\ell \sim \sqrt{D\tau}$.
- For a $p = 1\ atm, H_2 + air$ laminar flame, the length scale where fast reaction balances diffusion is $\sim 2\ \mu m$, the necessary scale for a DNS.

Part III: DNS of Complex Inert and Reacting Flows

Project Summary

- An adaptive method is applied to the simulation of compressible reacting flow.
- Model includes detailed chemical kinetics, multi-species transport, momentum and energy diffusion.
- Problems are typically multi-dimensional and contain a wide range of spatial and temporal scales.
- Method resolves the range of scales present, while greatly reducing required computational effort and automatically produces verified solutions.

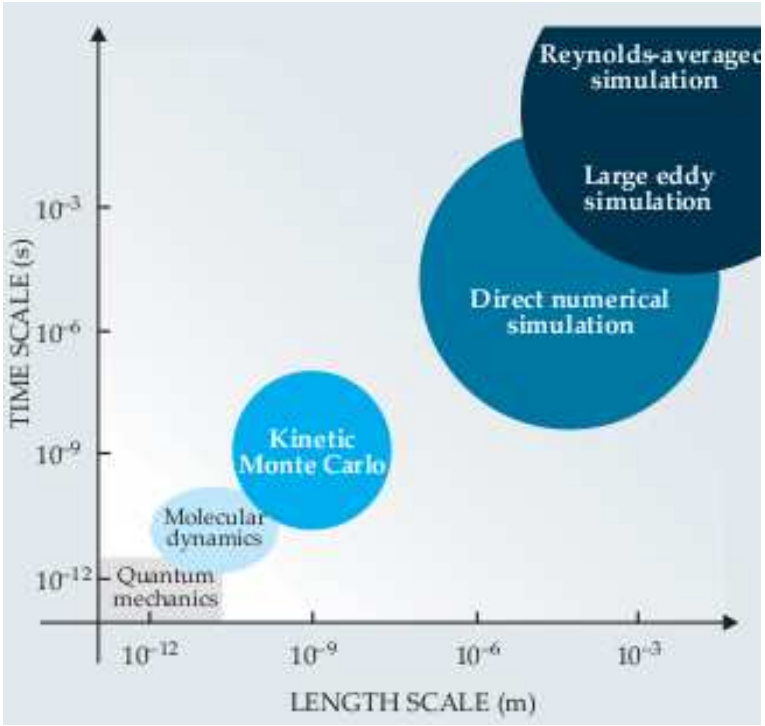

"Research needs for future internal combustion engines,"
Physics Today, Nov. 2008, pp 47-52.

Compressible Reactive Flow

Code solves the n-D compressible reactive Navier-Stokes equations:

$$\begin{aligned}
\frac{\partial \rho}{\partial t} &= -\frac{\partial}{\partial x_i}(\rho u_i) \\
\frac{\partial \rho u_i}{\partial t} &= -\frac{\partial}{\partial x_j}(\rho u_j u_i) - \frac{\partial p}{\partial x_i} + \frac{\partial \tau_{ij}}{\partial x_j} \\
\frac{\partial \rho E}{\partial t} &= -\frac{\partial}{\partial x_j}(u_j(\rho E + p)) + \frac{\partial u_j \tau_{ji}}{\partial x_i} - \frac{\partial q_i}{\partial x_i} \\
\frac{\partial \rho Y_k}{\partial t} &= -\frac{\partial}{\partial x_i}(u_i \rho Y_k) + M_k \dot{\omega}_k - \frac{\partial j_{i,k}}{\partial x_i}, \qquad k = 1, \ldots, K-1
\end{aligned}$$

Where ρ-density, u_i-velocity vector, E-specific total energy, Y_k-mass fraction of species k, τ_{ij}-viscous stress tensor, q_i-heat flux, $j_{i,k}$-species mass flux, M_k-molecular weight of species k, and $\dot{\omega}_k$-reaction rate of species k.

Compressible Reactive Flow (cont.)

Where,

$$\sum_{k=1}^{K} Y_k = 1$$

$$E = e + \frac{1}{2} u_i u_i$$

$$\tau_{ij} = -\frac{2}{3}\mu \frac{\partial u_l}{\partial x_l}\delta_{ij} + \mu\left(\frac{\partial u_i}{\partial x_j} + \frac{\partial u_j}{\partial x_i}\right)$$

$$q_i = -\mathsf{k}\frac{\partial T}{\partial x_i} + \sum_{k=1}^{K}\left(h_k j_{i,k} - \frac{RT}{m_k X_k} D_k^T d_{i,k}\right)$$

$$j_{i,k} = \frac{\rho Y_k}{X_k \overline{M}} \sum_{j=1, j\neq k}^{K} M_j D_{jk} d_{i,j} - \frac{D_k^T}{T}\frac{\partial T}{\partial x_i}$$

$$d_{i,k} = \frac{\partial X_k}{\partial x_i} + (X_k - Y_k)\frac{1}{p}\frac{\partial p}{\partial x_i}$$

Wavelet Approximation in Domain $[0,1]^d$

Approximation of $u(\mathbf{x})$ by the interpolating wavelet, a multiscale basis, on $\mathbf{x} \in [0,1]^d$ is given by

$$u(\mathbf{x}) \approx u^J(\mathbf{x}) = \sum_{\mathbf{k}} u_{j_0,\mathbf{k}} \Phi_{J_0,\mathbf{k}}(\mathbf{x}) + \sum_{j=J_0}^{J-1} \sum_{\lambda} d_{j,\lambda} \Psi_{j,\lambda}(\mathbf{x}),$$

where $\mathbf{x} \in \mathbb{R}^d$, $\lambda = (\mathbf{e}, \mathbf{k})$ and $\Psi_{j,\lambda}(\mathbf{x}) \equiv \Psi^{\mathbf{e}}_{j,\mathbf{k}}(\mathbf{x})$.

- Scaling function:
$$\Phi_{j,\mathbf{k}}(\mathbf{x}) = \prod_{i=1}^{d} \phi_{j,\mathbf{k}}(x_i), \ k_i \in \kappa_j^0$$

- Wavelet function:
$$\Psi^{\mathbf{e}}_{j,\mathbf{k}}(\mathbf{x}) = \prod_{i=1}^{d} \psi^{e_i}_{j,\mathbf{k}}(x_i), \ k_i \in \kappa_j^{e_i}$$

where $\mathbf{e} \in \{0,1\}^d \setminus \mathbf{0}$, $\psi^0_{j,k}(x) \equiv \phi_{j,k}(x)$ and $\psi^1_{j,k}(x) \equiv \psi_{j,k}(x)$, and $\kappa_j^0 = \{0, \cdots, 2^j\}$ and $\kappa_j^1 = \{0, \cdots, 2^j - 1\}$.

Sparse Wavelet Representation (SWR) and Irregular Sparse grid

- For a given threshold parameter ε, the multiscale approximation of a function $u(\mathbf{x})$ can be written as

$$u^J(\mathbf{x}) = \sum_{\mathbf{k}} u_{j_0,\mathbf{k}} \Phi_{j_0,\mathbf{k}}(\mathbf{x}) + \sum_{j=j_0}^{J-1} \sum_{\{\boldsymbol{\lambda} \,:\, |d_{j,\boldsymbol{\lambda}}| \geq \varepsilon\}} d_{j,\boldsymbol{\lambda}} \Psi_{j,\boldsymbol{\lambda}}(\mathbf{x})$$

$$+ \underbrace{\sum_{j=j_0}^{J-1} \sum_{\{\boldsymbol{\lambda} \,:\, |d_{j,\boldsymbol{\lambda}}| < \varepsilon\}} d_{j,\boldsymbol{\lambda}} \Psi_{j,\boldsymbol{\lambda}}(\mathbf{x})}_{R_\varepsilon^J},$$

  and the SWR is obtained by discarding the term R_ε^J.

- For interpolating wavelets, each basis function is associated with one dyadic grid point, *i.e.*

$$\Phi_{j,\mathbf{k}}(\mathbf{x}) \quad \text{with} \quad \mathbf{x}_{j,\mathbf{k}} = (k_1 2^{-j}, \ldots, k_d 2^{-j})$$

$$\Psi_{j,\lambda}(\mathbf{x}) \quad \text{with} \quad \mathbf{x}_{j,\boldsymbol{\lambda}} = \mathbf{x}_{j+1,2\mathbf{k}+\mathbf{e}}$$

SWR and Irregular Sparse Grid (continued)

- For a given SWR, one has an associated grid composed of *essential* points, whose wavelet amplitudes are greater than the threshold parameter ε

$$\boldsymbol{\mathcal{V}}_e = \{\mathbf{x}_{j_0,\mathbf{k}}, \bigcup_{j \geq j_0} \mathbf{x}_{j,\boldsymbol{\lambda}} \ : \ \lambda \in \boldsymbol{\Lambda}_j\}, \quad \boldsymbol{\Lambda}_j = \{\lambda \ : \ |d_{j,\lambda}| \geq \varepsilon\}.$$

- To accommodate the possible advection and sharpening of solution features, we determine the *neighboring* grid points:

$$\boldsymbol{\mathcal{V}}_b = \bigcup_{\{j,\boldsymbol{\lambda} \in \boldsymbol{\Lambda}\}} \mathcal{N}_{j,\boldsymbol{\Lambda}},$$

where $\mathcal{N}_{j,\boldsymbol{\lambda}}$ is the set of neighboring points to $x_{j,\boldsymbol{\lambda}}$.

- The new sparse grid, $\mathcal{V}$, is then given by

$$\boldsymbol{\mathcal{V}} = \mathbf{x}_{j_0,k} \cup \boldsymbol{\mathcal{V}}_e \cup \boldsymbol{\mathcal{V}}_b.$$

SWR and Irregular Sparse grid (continued)

- There exists an adaptive fast wavelet transform ($AFWT$), with $O(N)$, $N = \dim\{\boldsymbol{\mathcal{V}}\}$ operations, mapping the function values on the irregular grid $\boldsymbol{\mathcal{V}}$ to the associated wavelet coefficients and *vice-versa*:

$$AFWT(\{u(\mathbf{x}) \,:\, \mathbf{x} \in \boldsymbol{\mathcal{V}}\}) \rightarrow \mathcal{D} = \{\{u_{j_0,\mathbf{k}}\}, \{d_{j,\boldsymbol{\lambda}},\ \boldsymbol{\lambda} \in \boldsymbol{\Lambda}_j\}_{j>j0}\}.$$

- Provided that the function $u(\mathbf{x})$ is continuous, the error in the SWR $u_\varepsilon^J(\mathbf{x})$ is bounded by

$$\|u - u_\varepsilon^J\|_\infty \leq C_1\ \varepsilon.$$

- Furthermore, for the function that is smooth enough, the number of basis functions $N = \dim\{u_\varepsilon^J\}$ required for a given ε satisfies

$$N \leq C_2\ \varepsilon^{-d/p}, \quad \text{and} \quad \|u - u_\varepsilon^J\|_\infty \leq C_2\ N^{-p/d}.$$

Derivative Approximation of SWR

- Direct differentiation of wavelets is costly (with $O(p(J-j_0)N)$ operations) because of different support sizes of wavelet basis on different levels.

- Alternatively, we use the connection with Lagrange interpolating polynomials to approximate the derivative on a grid of irregular points. The procedure can be summarized as follows:

  1. For a given SWR of a function, perform the inverse interpolating wavelet transform to obtain the function values at the associated irregular points.
  2. Apply locally a finite difference scheme of order n to approximate the derivative at each grid point.

- Estimate shows that the pointwise error of the derivative approximation has the following bound:

$$\|\partial^i u/\partial x^i - D_x^{(i)} u_\varepsilon^J\|_{\boldsymbol{\nu},\infty} \leq C N^{-\min((p-i),n)/2}, \quad \|f\|_{\mathcal{G},\infty} = \max_{\mathbf{x}\in\boldsymbol{\nu}} |f(x)|.$$

Dynamically Adaptive Algorithm for Solving Time-Dependent PDEs

Given the set of PDEs

$$\frac{\partial u}{\partial t} = F(t, u, u_x, u_{xx}, \ldots),$$

with initial conditions

$$u(x, 0) = u^0.$$

1. Obtain sparse grid, $\boldsymbol{\nu}^m$, based on thresholding of magnitudes of wavelet amplitudes of the approximate solution u^m.
2. Integrate in time using an explicit time integrator with error control to obtain the new solution u^{m+1}.
3. Assign $u^{m+1} \rightarrow u^m$ and return to step 1.

Parallelization

- Parallel algorithm uses an MPI-based domain decomposition.
- Hilbert space-filling curve used for partitioning and load-balancing.
- Strong scaling up to 256 cores with $> 90\%$ parallel efficiency.
- Chemkin-II and Transport Libraries used for evaluation of thermodynamics, transport properties, and reaction source terms.

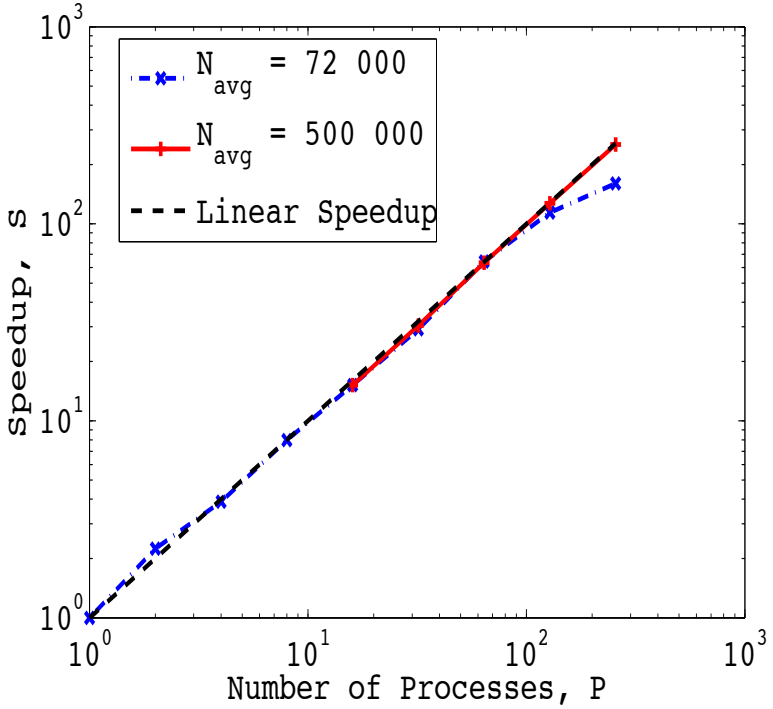

Dual Quad-Core, 2.7 GHz L5520 Intel Nehalem nodes (8 cores/node), 12 GB RAM, Infiniband interconnect

2-D Viscous Detonation

Initial Conditions:

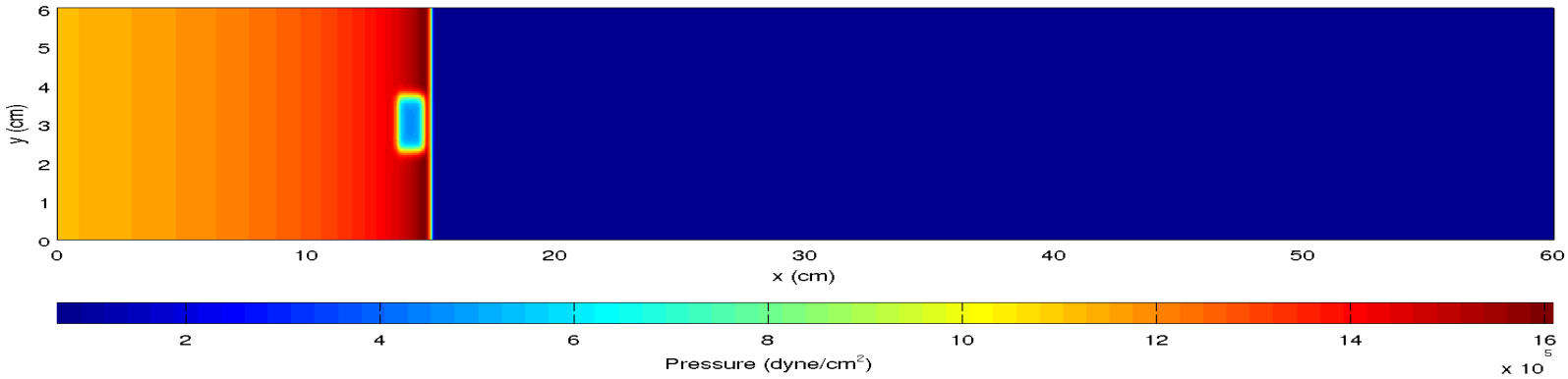

Domain: $[0, 60] \times [0, 6]$ cm
Front: $x = 15.0$ cm
Unreacted pocket:
$[1.05 \times 1.43]$ cm
at $x = 14.7$ cm
$P = 4.7 \times 10^5$ dyne/cm^2
$T = 2100$ K
128 cores
391 hrs runtime

$2H_2 : O_2 : 7Ar$ mixture
9 species, 37 reactions

Wavelet parameters:
$\epsilon = 1 \times 10^{-3}$
$p = 6, \quad n = 5$
$[N_x \times N_y]_{j_0} = [600 \times 60]$
$J - j_0 = 10$

2-D Viscous Detonation (cont.)

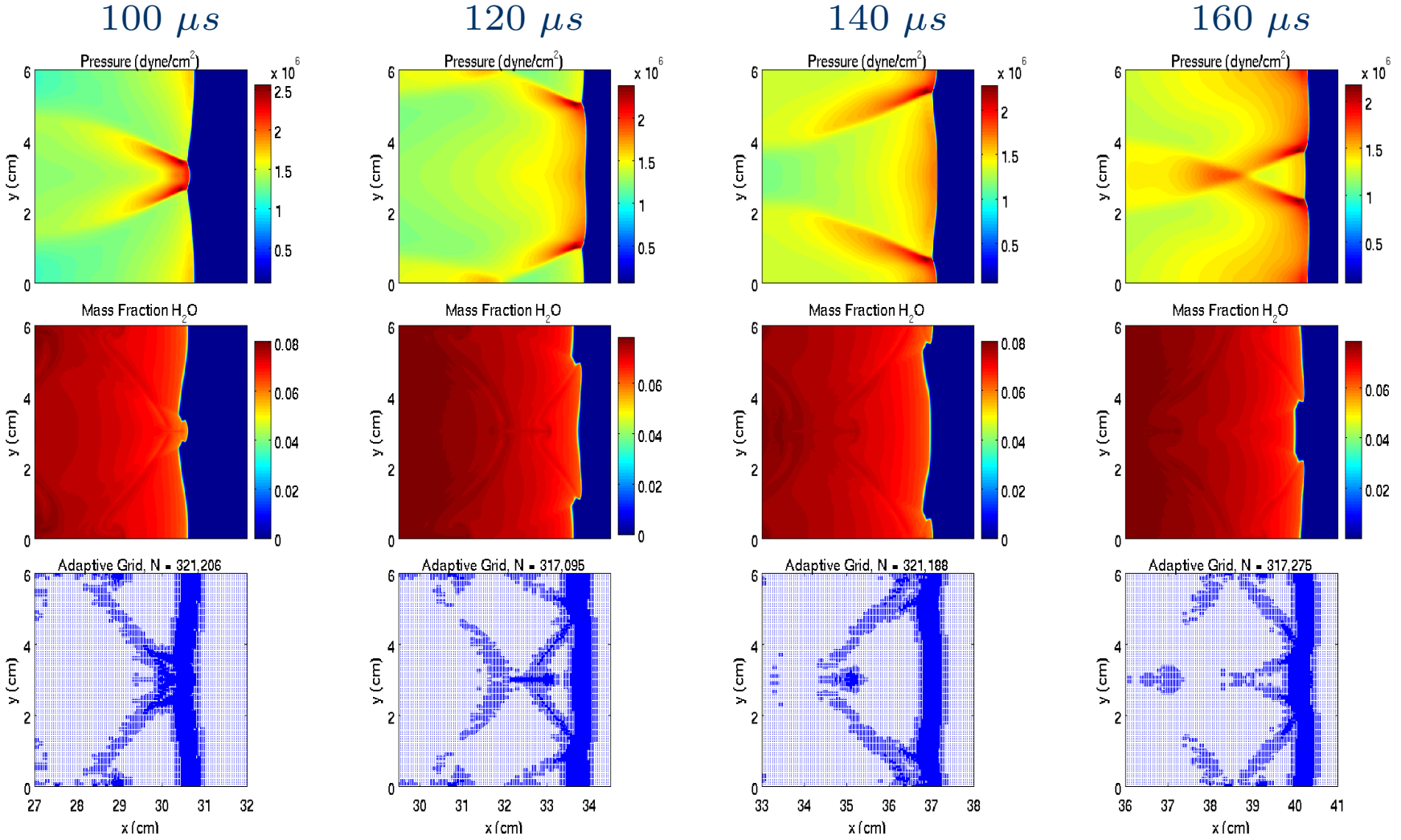

2-D Viscous Detonation (cont.)

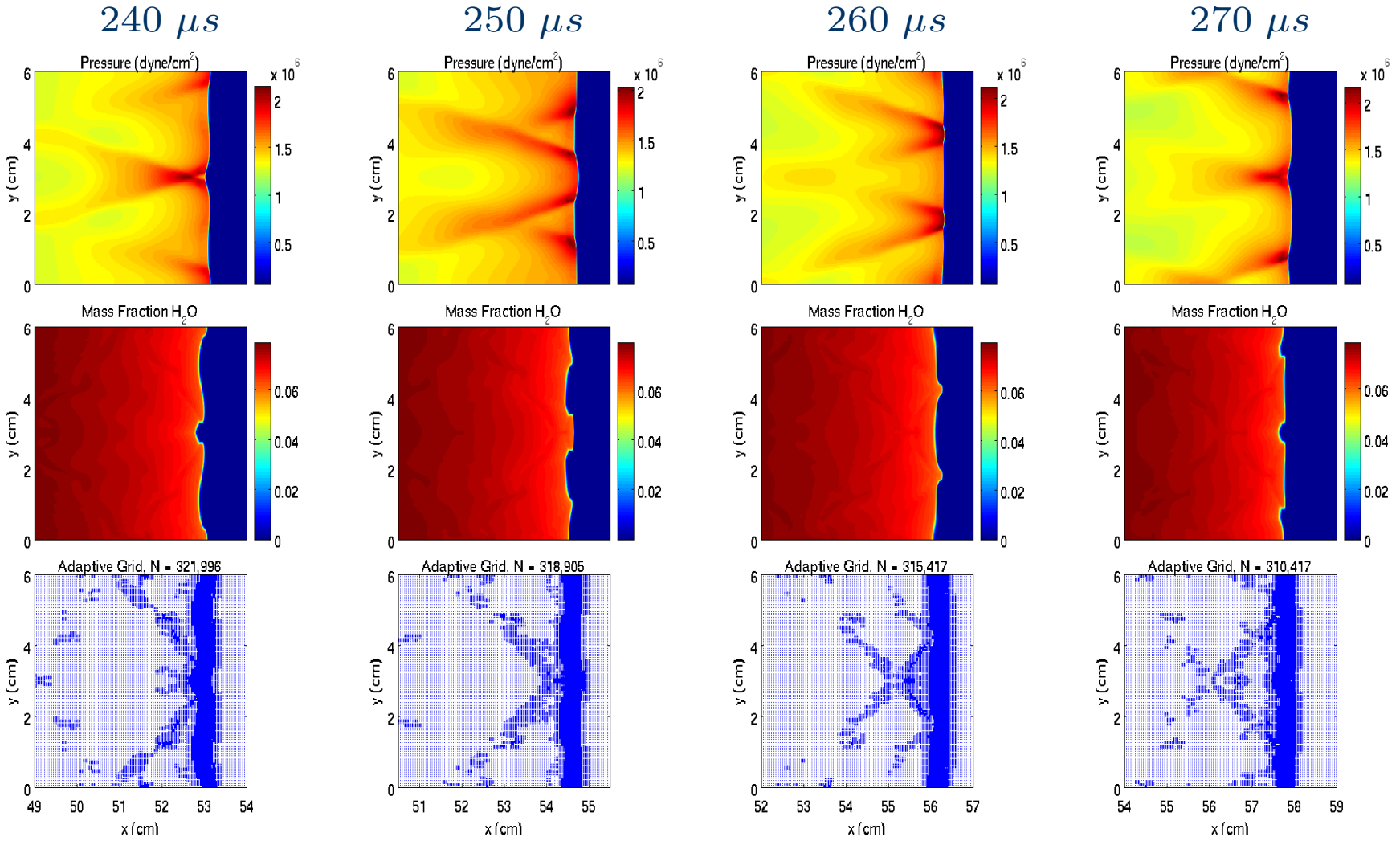

Shock/H_2-Bubble Interaction

Initial Conditions:

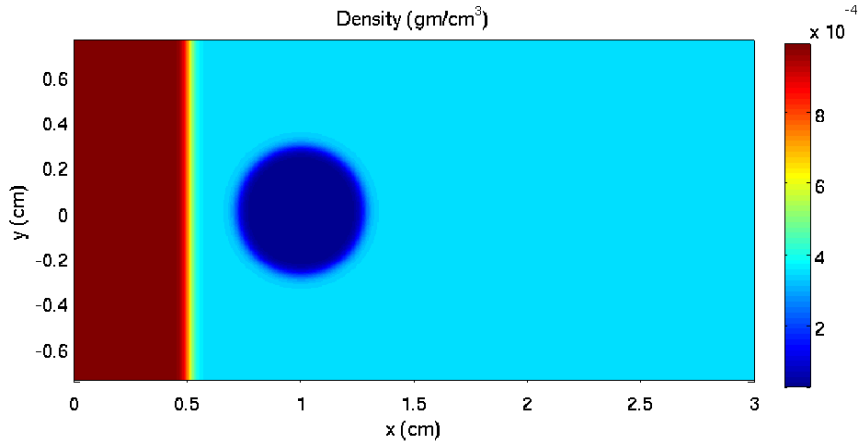

Domain: $[0, 3] \times [0, 0.75]$ cm
Mach 2 shock: $x = 0.5$ cm
$P_\infty = 1.0 \times 10^6$ dyne/cm^2
$T_\infty = 1000$ K
$r = \sqrt{(x-1)^2 + y^2}$
$r < 0.28$ cm: $83H_2 : 17N_2$
$r > 0.28$ cm: $22O_2 : 78N_2$
64 cores
runtime

$H_2 : O_2 : N_2$ mixture
9 species, 37 reactions

Wavelet parameters:

$\epsilon = 1 \times 10^{-3}$
$p = 6, \quad n = 5$
$[N_x \times N_y]_{j_0} = [30 \times 8]$
$J - j_0 = 10$

Shock/H_2-Bubble Interaction (cont.)

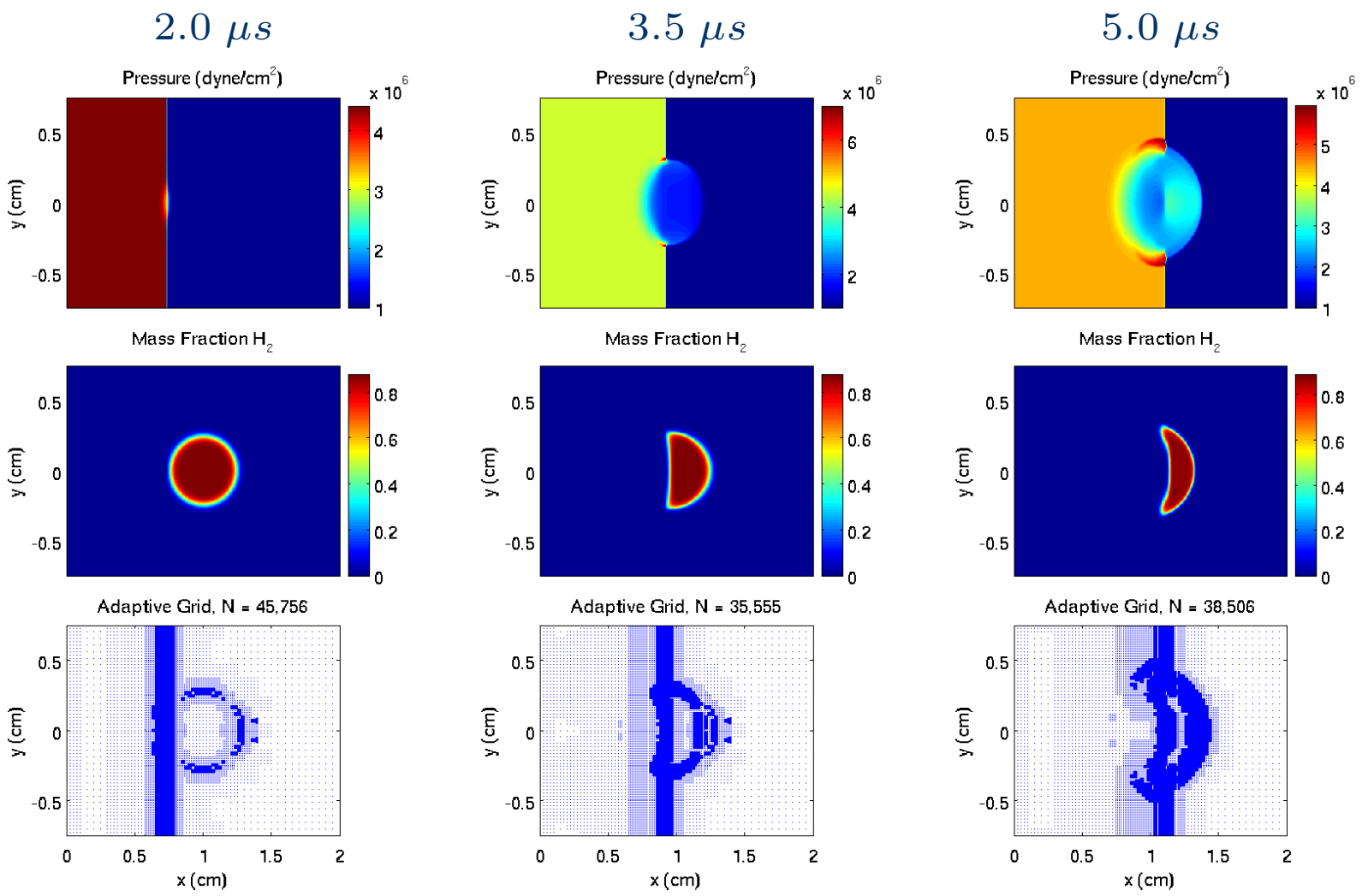

Richtmeyer-Meshkov Instability

Initial Conditions:

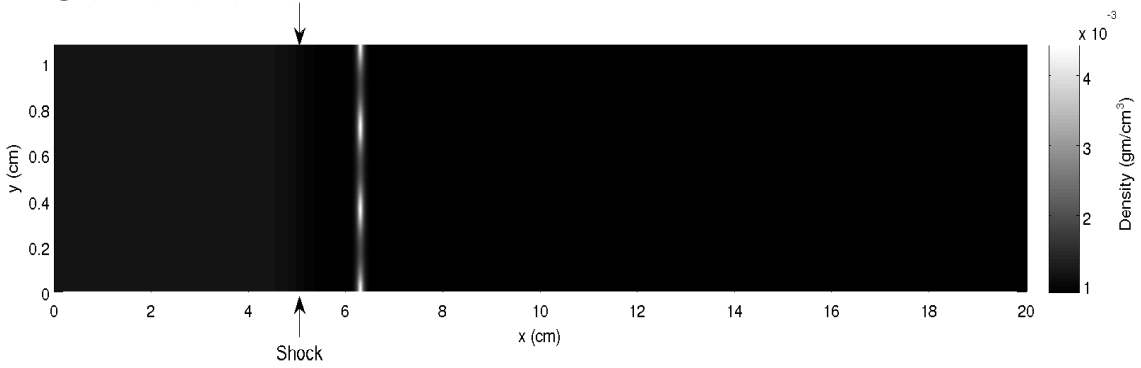

Domain:
$[0, 20] \times [0, 1.08]$ cm

Ambient mixture:
$Y_{N_2} = 0.99,\ Y_{SF_6} = 0.01$
$P = 79.5$ kPa
$T = 300$ K

$M_s = 1.2$ shock
at $x = 5.0$ cm

64 cores

118 hrs runtime

Varicose sheet at $x = 6.3$ cm
$Y_{N_2} = 0.01,\ Y_{SF_6} = 0.99$
Balakumar *et al.*
Phys. Fluids **20**, 2008

Wavelet parameters:
$\epsilon = 1 \times 10^{-4}$
$p = 6, \quad n = 5$
$[N_x \times N_y]_{j_0} = [200 \times 10]$
$J - j_0 = 10$

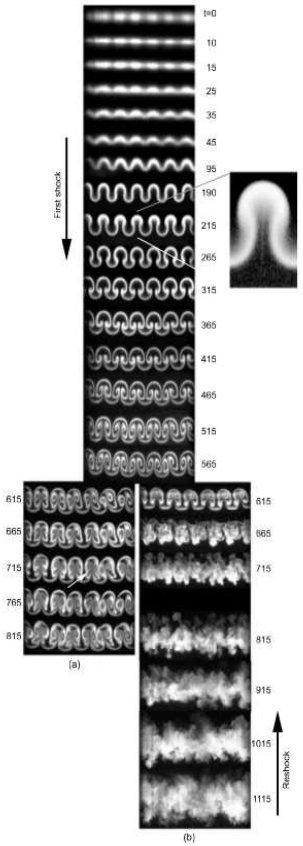

Richtmeyer-Meshkov Instability (cont.)

$\Longrightarrow$ Shock Direction $\Longrightarrow$

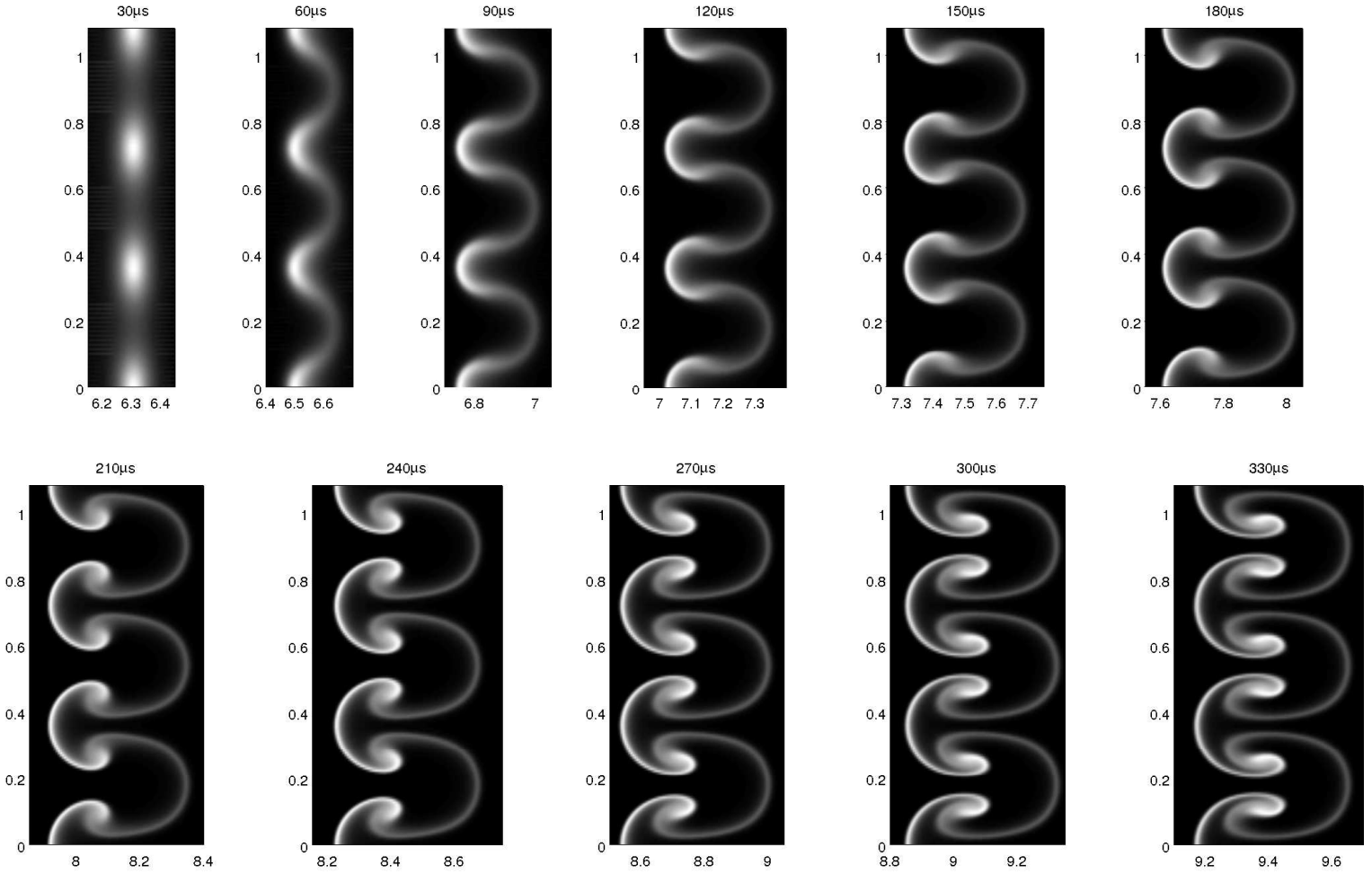

Richtmeyer-Meshkov Instability (cont.)

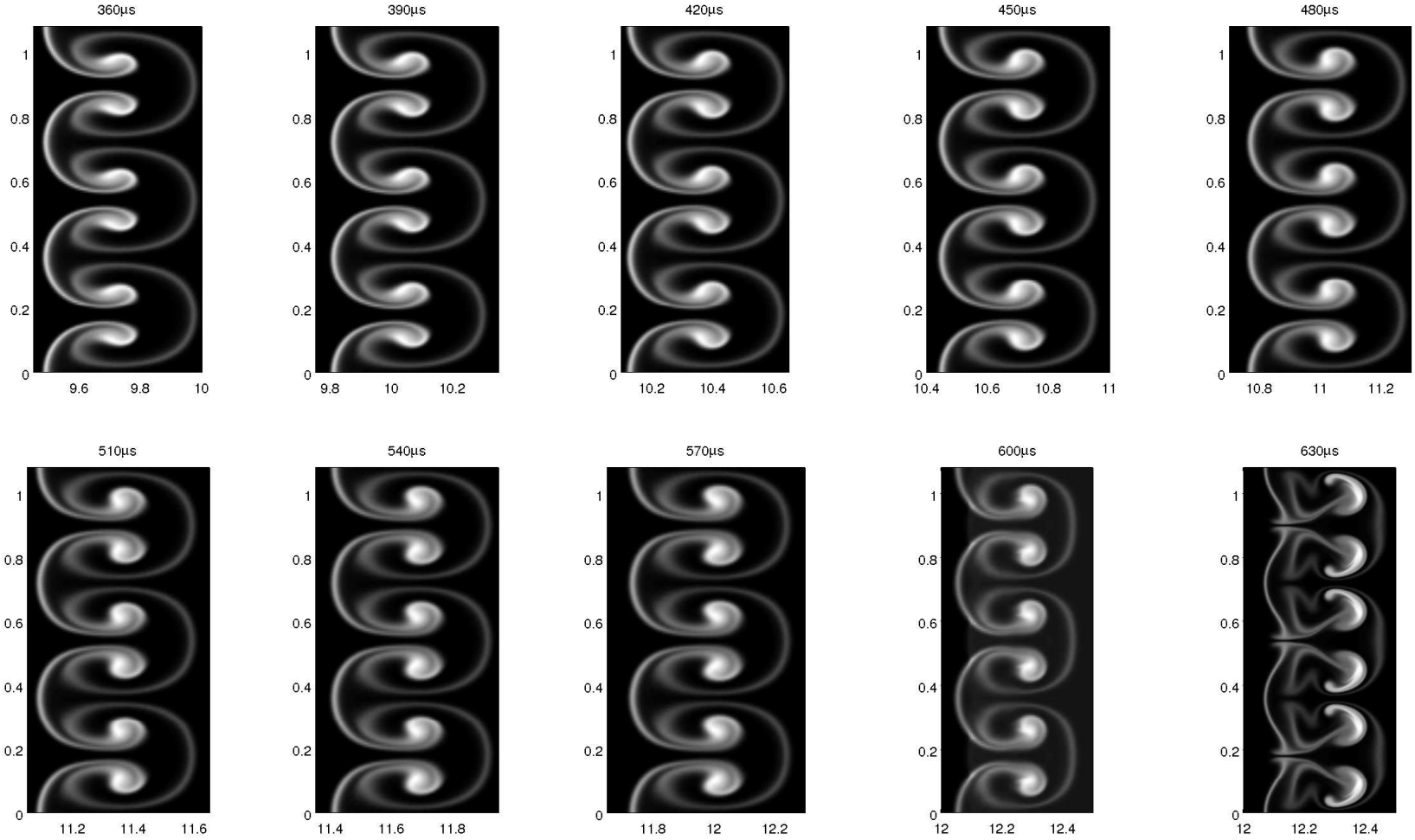

⇐ Reshock ⇐

Richtmeyer-Meshkov Instability – Grid

$t = 390\ \mu s$ $t = 600\ \mu s$

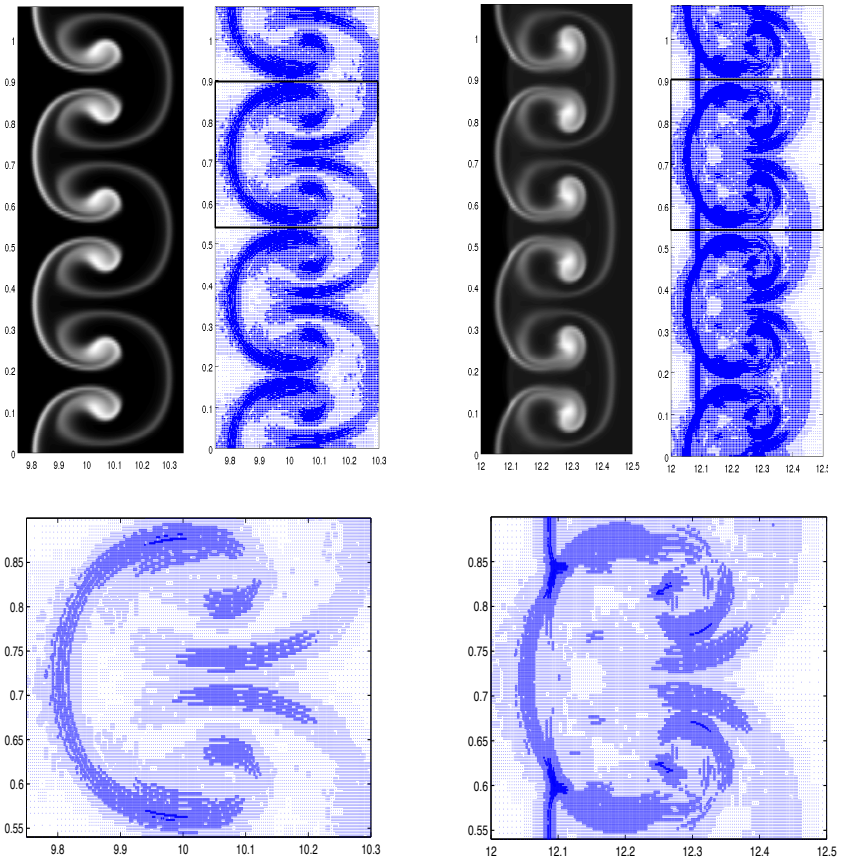

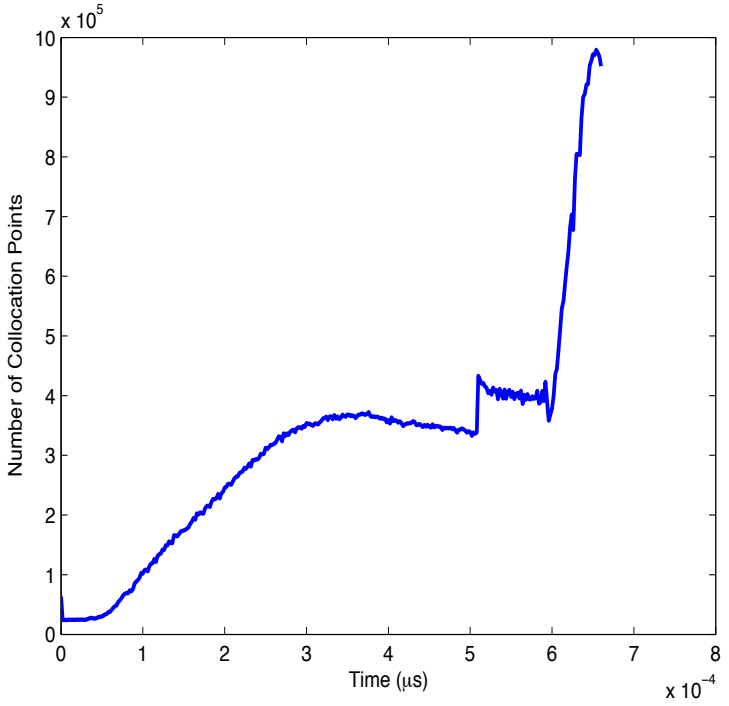

Effect of Diffusion on Long-Time Detonation Dynamics

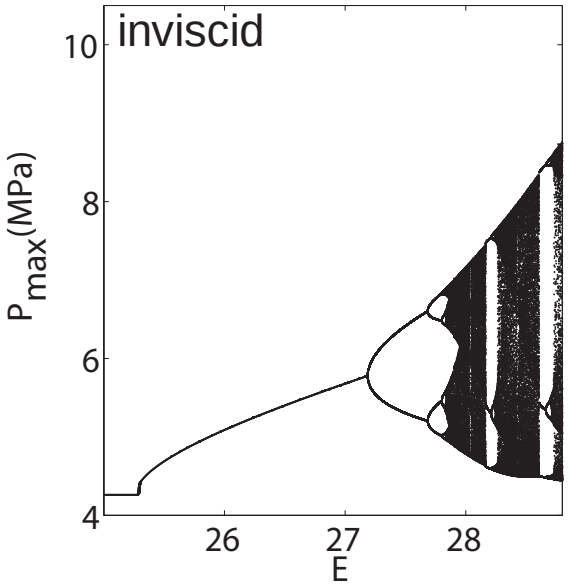

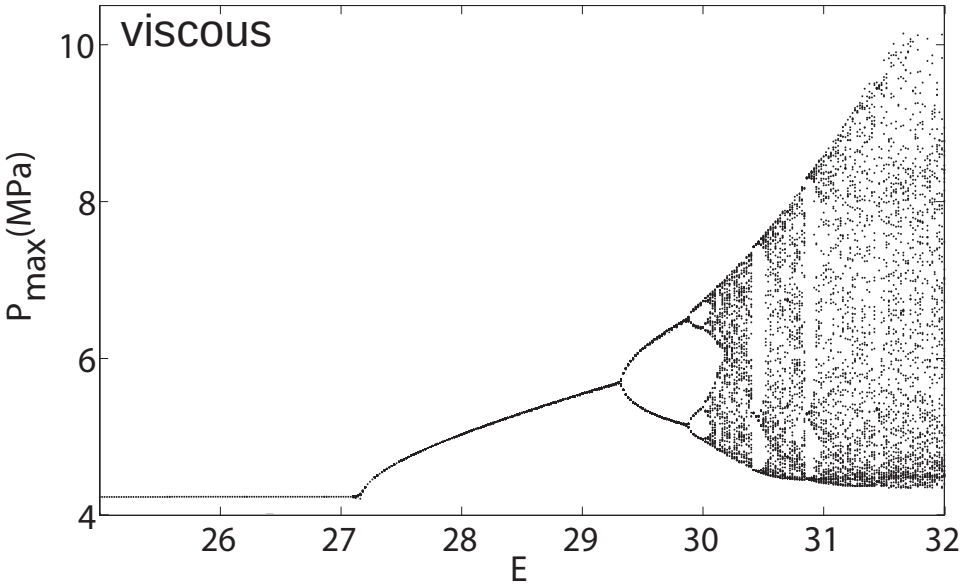

- Standard 1D problem with one-step kinetics, see Powers, *et al.*, 2006.
- Small physical diffusion significantly delays transition to instability.
- In the unstable regime, small diffusion has a large role in determining role for the long time dynamics.

Inert Viscous Cylindrical Implosion

- $100\ \mu m \times 100\ \mu m$ square domain,
- Pure argon,
- Initial uniform temperature, $T = 300\ K$,
- Initial pressure ratio is $4\ atm : 0.2\ atm$ between argon on either side of an octagonal diaphragm,
- $T_{max}(r = 0, t \sim 40\ ns) \sim 2400\ K$.

Conclusions

- Verified 2D calculations for realistic reacting gas mixtures with detailed kinetics and multicomponent transport are realizable with modern adaptive algorithms working within a massively parallel computing architecture.
- It is possible for 2D calculations to span over five orders of magnitude: from near mean-free path scales ($10^{-4}\ cm$) to small scale device scales ($10\ cm$).
- Micro-scale viscous shock dynamics can dramatically influence oscillatory detonation dynamics on the macro-scale (see Romick, *et al.*, 2011).
- Validation against unsteady calculations awaits 3D extensions.
- Realization of verified and validated DNS would remove the need for common, but problematic, modeling assumptions (shock-capturing, turbulence modeling, implicit chemistry with operator splitting, reduced kinetics/flamelets).
- Such 3D V&V could be viable in an exascale environment; however, routine desktop DNS calculations remain difficult to envision at macro-device scales.

An Advertisement:

- Workshop on Verification and Validation in Computational Science
- 17-19 October 2011
- on the ND campus
- limited NSF travel support available for young researchers
- `http://vv.nd.edu`